SYNTHESIS OF LANTHANIDE MOLYBDATES VIA REACTION OF MOLYBDENUM(VI) OXIDE WITH AQUEOUS ACETATE SALTS

By
KHALID ALRASHIDI
Bachelor of Science in Chemistry
King Saud University
Riyadh, Saudi Arabia 2012

Submitted to the Faculty of the
Graduate College of the
Oklahoma State University
in partial fulfillment of
the requirements for
the Degree of
MASTER OF CHEMISTRY
DECEMBER 2018

SYNTHESIS OF LANTHANIDE MOLYBDATES VIA REACTION OF MOLYBDENUM(VI) OXIDE WITH AQUEOUS ACETATE SALTS

Thesis Approved:

Dr. Allen W. Apblett

Thesis Adviser

Dr. Nicholas F. Materer

Dr. Gabriel Cook

ACKNOWLEDGEMENTS

Thanks to merciful Allah for all the countless gifts you have offered and thanks to my family and my friends for their love and support. My deepest thanks and gratitude to my mother for her extraordinary support, prayers, and unconditional love.

It is a great pleasure to acknowledge my deepest thanks to my adviser Prof. Allen Apblett. I am thankful for Professor Apblett, a faculty member at Oklahoma State University, for his encouragement, creative, and comprehensive advice until this research work came to existence. It is a great honor to work under his supervision. This thesis would not have been possible without the help, support and patience of my principal advisor Prof. Apblett, which I am extremely grateful. Also, I would like to thank Prof. Nicholas F. Materer and Dr. Gabriel Cook for their advice and help.

I would also like to express my extreme sincere gratitude and appreciation to all my Saudi Arabian Cultural Mission (SACM) as well as King Saud University for sponsoring and supporting.

TABLE OF CONTENTS

LIST OF TABLES

CHAPTERII **Page**

LIST OF FIGURES

CHAPTER I **Page**

CHAPTER II

CHAPTER I

Introduction

Introduction

The chemistry of molybdenum is important due to its ability to form complexes with valence states 0, +1, +2, +3, +4, +5, and +6. Molybdenum trioxide, with +6 oxidation state is particularly important to chemists to form lanthanide molybdate. Molybdenum is in Group VI of the periodic table and is located in the 4d-block between Nb and Tc. It is a very refractory metal with an extremely high melting point of 2610 ℃. For this reason, molybdenum can be used as a high strength material in the high temperature conditions. Molybdenum has conductivity, so it can be used as an electrical material for so many applications. Molybdenum slowly oxidizes in air at 350 ℃ but it is rapidly oxidized at 650 ℃ and above.

Molybdenum compounds have a wide range of applications. For instance, they are used in such technological areas as catalysis, lubrications, refractories, paints, and allied industries. For instance, liquid and MoS_2 can be utilized to prepare lubricants in both form.[5] Over the

past decade, molybdenum has expanded into other markets that employ the extraordinary characterizations of this many-sided element.[5-14]

Molybdenum Trioxide

The structure of molybdenum trioxide

The molybdenum oxides are noted for their very rich chemistry and multiple structures. For instance, the binary oxides include the dioxide and the trioxide as well as an extensive series of intermediate phases with the general formula Mo_nO_{3n-m}. However, the ternary oxides are more extensively because of their versatility ranging from complex polymolybdates based on Mo^{VI} to metal cluster compounds with molybdenum in oxidation states as low as 2.5.

Molybdenum trioxide adopts the layered α-structure shown in (Figure 1.1). It is a fascinating and important material as well as the ultimate oxidation product of most molybdenum compounds. The color of the molybdenum trioxide is a pale yellow. It sublimes at temperatures above 700 ℃ to produce a vapor that contains cyclic Mo_3O_9, Mo_4O_{12} and Mo_5O_{15} clusters that are based on corner shared MoO_4 tetrahedra. In most materials, molybdenum oxide is most likely to have either tetrahedral or octahedral coordination, but in the α-MoO_3, the molybdenum environment is square pyramidal within the layer of the structure (Mo-O bond lengths of 1.67, 1.73, 2*1.95 and 2.25 A˚), with a more distant sixth oxygen from an adjacent layer forming highly distorted octahedron (Mo-O bond length of 2.33A˚)

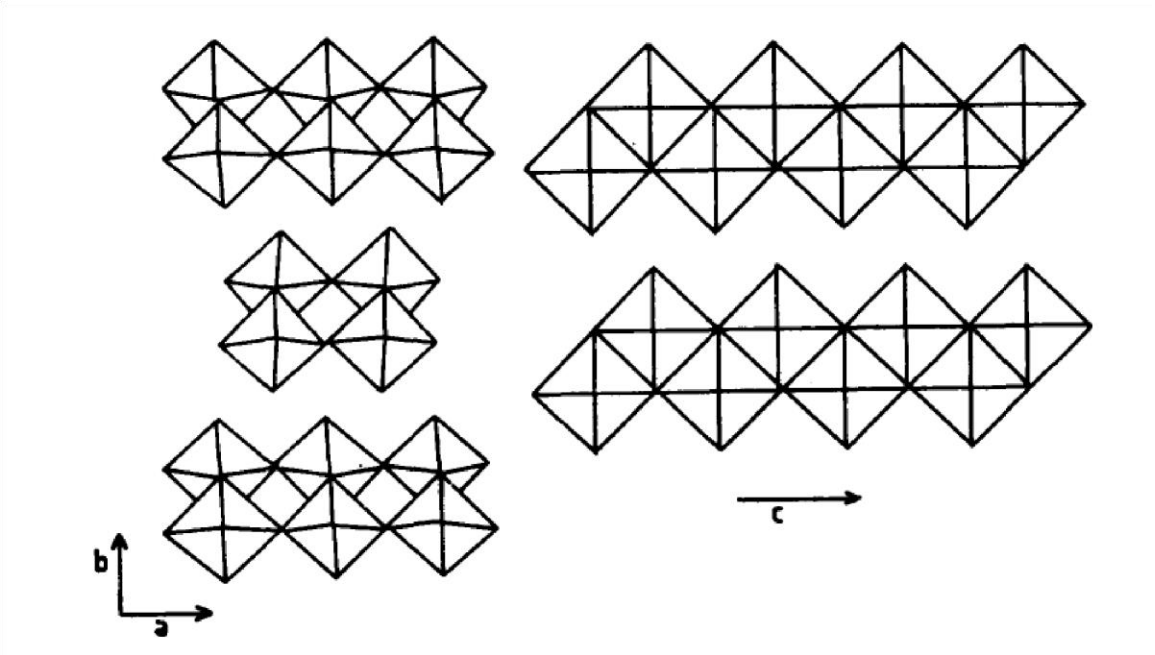

Figure 1.1. Idealized representation of the layered structure of molybdenum trioxide as reported by Chippendale and Cheatham[1]

Moreover, MoO_3 and its hydrates are soluble in alkaline solutions since they react to form soluble molybdate(VI) ions. MoO_3 can also be reacted with DMSO, pyridine and methanol to form isopolymolybdates.[1] The molybdenum compounds have higher activities for the water-gas shift reaction than nickel and iron except MoS_2 and MoO_3.[15]

Lanthanide Molybdate Oxide Conductors

Lanthanide molybdate is solid oxides to conduct ions and fast oxide-ion conductors (or oxide electrolytes) are used for several purposes ranging from oxide fuel cells to oxygen purification isolation. For practical purposes, these oxide electrolytes have to have high oxide-ion mobility at low operating temperatures. High mobility can be found for materials that possess certain structural aspects because of the size of the cations and the interaction of oxygen ions with the cationic network. Thus, high oxide ion mobility has only been

observed in a small number of structural types includes as fluorite, perovskite; intergrowth perovskite/Bi_2O_2 layers, and pyrochlores. A class of solid oxides based on, $La_2Mo_2O_9$ (that has with a different crystal structure from all known oxide electrolytes) shows fast oxide-ion conducting characteristics. Furthermore, the material has a structural transition around 580 ℃ that leads to an increase in conductivity by approximately two orders of magnitude. The similar structure of $La_2Mo_2O_9$ to β-$SnWO_4$ suggests a structural model for the origin of the oxide-ion conductivity. In general, replacement of a cation that has a lone pair of electrons by a different cation that does not have a lone pair and has a higher oxidation state can be used as a method to make novel oxide-ion conductors.[16-29]

Lanthanide Molybdates

Synthesis of Lanthanide Molybdates and Characterization Methods

One might expect the facile synthesis of lanthanide molybdates by a precipitation reaction between aqueous lanthanide metal salt and aqueous sodium molybdate as shown in Scheme 1. However this metathesis reaction usually fails to produce the ortho molybdates, $Ln_2(MoO_4)_3$, due to preferential formation of $NaLn(MoO_4)_2$. Furthermore such reactions are not suited for the synthesis of other useful lanthanide molybdenum oxide bimetallic oxide phases such as $Ln_2Mo_2O_9$ and Ln_2MoO_6.

$$3\ Na_2MoO_{4(aq)} + 2\ LnCl_{3(aq)} \rightarrow Ln_2(MoO_4)_{3(s)} + 6\ NaCl_{(aq)}$$

$$2Na_2MoO_{4(aq)} + LnCl_{3(aq)} \rightarrow NaLn(MoO_4)_{3(s)} + 3\ NaCl_{(aq)}$$

Scheme 1. Aqueous Metathesis Reactions of Lanthanide Salts with Sodium Molybdate

The Apblett group discovered an alternative for the synthesis of lanthanum molybdenum oxide phases in aqueous media during an investigation of the usefulness of molybdenum trioxide for the removal of metal ions from simulated radioactive waste. Molybdenum oxide has a layered structure composed of chains of edge-shared distorted MoO_6 octahedra that are interconnected through corner linking to form infinite chains [2]. These chains are further linked by edge-sharing to form double-layer sheets. The sheets stack together via Van der Waals forces to give the final layered structure (Figure 1.2). Based on this structure, the Apblett research group decided to explore the possibility that intercallation of metals between the sheets followed by a reaction to form molybdate phases would be a promising approach for immobilization of radionuclides from nuclear waste [30-33].

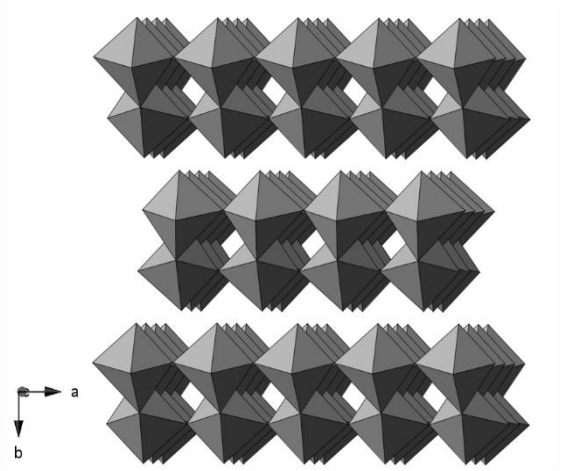

Figure 1.2. Layered Structure of MoO_3 (Drawn using Crystal Maker X and crystallographic data from Reference [2])

It was discovered that the reaction of MoO_3 with aqueous uranyl failed to go to completion due to a sharp decrease in pH as protons were produced according to Equation 1[93131]. Therefore, an acetic-acid/acetate buffer was used (pH=4.75) so that reactions could proceed to completion. Later, a strategy of using metal acetates instead of chlorides was adopted so that over-acidification was prevented by reaction of acetate ions with protons to form acetic acid, a weak acid with a pKa of 4.75. Notably, if a sufficient excess of metal acetate is used in these reactions, the reaction mixture will be self-buffered since a mixture of acetic acid and its conjugate base will be produced.

$$MoO_{3(s)} + H_2O_{(l)} \longrightarrow MoO_4^{2-}{}_{(aq)} + 2\ H^+{}_{(aq)} \qquad (1)$$

Chehbouni and Apblett performed a prolonged reaction of molybdenum trioxide with an aqueous solution of uranyl acetate to determine the maximum uptake of uranium and identify the product of the reaction [32]. The ratio of MoO_3 to UO_2^{2+} used was 1:1.43. Over a period of one week, the MoO_3 absorbed 165% by weight of uranium. This equated to 6.94 millimoles of uranium per gram of MoO_3 and, therefore, a 1:1 ratio of molybdenum to uranium. The product had the characteristic yellow color of hexavalent uranium and its infrared spectrum was consistant with the formation of a hydrated compound containing uranyl ions and molybdenum oxide octahedra. This was confirmed by X-ray powder diffraction that identified the product as the mineral umohoite, $(UO_2)MoO_4(H_2O)_2$. Heating of this product to 600˚C produced phase-pure $UMoO_6$. The reaction between uranyl ions and molybdenum trioxide performed at pH 4.7 in a 0.1 M acetic acid/acetate buffer was found to be first order in both reactants (Equation 2) with a rate constant, k, of 0.084 L/mol·min.[9] Note that the "concentration" of solid MoO_3 is represented as molarity in Equation 2.

$$\text{Rate} = k[MoO_3][UO_2^{2+}] \qquad (2)$$

The reaction of metal acetates with molybdenum trioxide to form hydrated bimetallic molybdenum oxide phases was extended to a wide range of divalent transition and lanthanide metals and it was found that this is a quite general reaction [31]. Relevant to the investigation reported herein is the reaction of aqueous gadolinium acetate with molybdenum trioxide [30]. This reaction was performed with 2:3 Gd:Mo molar ratio at reflux for seven days using 0.10 M gadolinium acetate. At the end of the reaction all of the

gadolinium had been absorbed from solution to yield a white solid. The formula of this product was determined to be $Gd_2(MoO_4)_3 \cdot 2.2H_2O$ (Equation 3). XRD analysis showed that the product was a crystalline phase but no match to known gadolinium or molybdenum phases could be found. Upon heating to 600˚C the solid was converted to $Gd_2Mo_3O_9$. When the reaction was performed with a molar ratio of 1:1 Gd:Mo, a different compound was formed with the formula $GdMoO_4(OH) \bullet 1.5H_2O$ (Equation 4). The product can be described as gadolinium molybdate hydroxide but the infrared spectrum indicates that it is not a true molybdate but contains molybdenum with a higher coordination number. A novel $Gd_2Mo_2O_9$ phase is produced upon heating to 550˚C. On the other hand, when, lanthanum acetate was reacted with MoO_3 under similar conditions, a lanthanum molybdate acetate, $La(MoO_4)(O_2CCH_3) \bullet H_2O$ was produced that served as a precursor for the oxide ion conductor, $La_2Mo_2O_9$, upon heating to 550˚C.

$$2\ Gd(O_2CCH_3)_3 + 3\ MoO_3 + 5.2H_2O \rightarrow Gd_2(MoO_4)_3 \cdot 2.2H_2O + 6\ CH_3CO_2H \quad (3)$$

$$Gd(O_2CCH_3)_3 + MoO_3 + 3.5\ H_2O \rightarrow GdMoO_4(OH) \bullet 1.5H_2O + 3\ CH_3CO_2H \quad (4)$$

$$La(O_2CCH_3)_3 + MoO_3 + 3\ H_2O \rightarrow La(MoO_4)(O_2CCH_3) \bullet H_2O + 2\ CH_3CO_2H \quad (5)$$

The purpose of this investigation was to determine what factors influence the formation of lanthanide molybdate hydroxides versus lanthanide molybdate acetates. The hypothesis was that the path of the reactions of molybdenum trioxide with lanthanide acetates was

dependent on the ionic radii of the lanthanide(III) ions. Thus, reactions were performed with yttrium, lanthanum, cerium, and praseodymium with different ionic radii (Figure1.3). This investigation also targeted the synthesis of new lanthanide phases with the formula $Ln_2Mo_2O_9$ that could be useful catalysts and oxide conductors. Also, the lanthanide ions do not affect the molybdate ion vibrational behavior. Finally, the lessons learned about the formation of lanthanide molybdate acetates were used to produce phosphors based on praseodymium-doped $La_2Mo_2O_9$. [34-42]

Y^{3+} **0.900**		
La^{3+} **1.032**	**Ce^{3+}** **1.010**	**Pr^{3+}** **0.990**

Figure1.3. Periodic Table Representation of the Metals Used in this Investigation and their Ionic Radii in Angstrom.[43]

CHAPTER II

ROUTES FOR THE SYNTHESIS OF LANTHANUM AND CERIUM MOLYBDATES CHARACERIZATION

Introduction

Recently, many chemists have been interested in the synthesis of rare earth molybdates $Ln_2(MoO_4)_3$ (where Ln can be lanthanum, cerium, gadolinium, praseodymium, yttrium, or any of the respective rare earth element in the periodic table).[44] $Ln_2Mo_2O_9$ is another ternary phase formed by lanthanides and molybdenum. These compounds have extensive applications as oxide conductors, phosphors, and catalysis. The use of molybdenum trioxide to remove lanthanides and actinides from water was described in Chapter 1. For example, it was reported that MoO_3 could absorb up 165% by weight of uranium, Umohite, a hydrated uranium molybdate.[44] The synthesis of lanthanide molybdates via reaction of molybdenum(VI) oxide with aqueous acetate salts was also reviewed in chapter 1. In this investigation, reaction of the aqueous solutions of either

lanthanum or cerium acetate with molybdenum(VI) oxide (MoO_3) was found to produce a mixed lanthanide molybdate acetate $Ln(O_2CCH_3(MoO_4))\bullet XH_2O$ where Ln can be either La or Ce. The products serve as excellent single source precursor for stoichiometric $La_2Mo_2O_9$ and $CeMoO_5$. The lanthanum molybdate acetate and cerium molybdate acetate were characterized by Fourier transform infrared spectroscopy (FT-IR), thermogravimetric analysis (TGA), NMR spectroscopy, X-Ray Powder Diffraction (XRD), and microwave plasma atomic emission spectroscopy (MP-AES). The conversion of the products to lanthanide molybdenum oxides is discussed along with the possibility of producing phosphors, $La_2Mo_2O_9:Ln^{3+}$ by doping lanthanum molybdenum oxides with other lanthanide metals such as praseodymium. The phosphor $La_2Mo_2O_9:Pr^{3+}$, and red light emitter, was previously prepared by high temperature solid state reaction from 800-900 °C[4]. In the previous work, optimal doping amount of Pr^{3+} was determined to be x=0.07 $La_{1-x}Pr_xMoO_{4.5}$. This phosphor was targeted in this investigation via the preparation of a praseodymium-doped lanthanum molybdate acetate and its thermal conversion to the corresponding oxide.[45-52]

Experimental

Reaction of molybdenum trioxide with lanthanum acetate

$La(CH_3CO_2)_3 \bullet 1.5\ H_2O$ (7.138 g, 20 mmol) was dissolved in 100 ml of distilled water in a round bottom flask. Next, molybdenum trioxide (MoO_3) (1.446 g, 10 mmol) was added to the solution of lanthanum acetate. The pH was determined to be 7 at the beginning of the reaction. The mixture was heated to reflux for nine days. After that, the reaction was placed on a bench to cool it down to room temperature. The lanthanum molybdate acetate was isolated by filtration and was washed extensively with water. At the of this time, the pH had fallen to 4.3. After drying in vacuum at room temperature for two days, a white solid later identified as $La(O_2CCH_3)(MoO_4) \bullet 1.05H_2O$ was isolated in a yield of 3.757 g 99.94 % based on the amount of MoO_3 used. Thermal gravimetric analysis (TGA) indicated the presence of 5.03 mass % water (Figure 2.1.) There was also a 13.93 % weight loss due to conversion of acetate ions to oxide ions. Heating $La(O_2CCH_3)(MoO_4) \bullet 1.05H_2O$ to 700 °C produced $La_2Mo_2O_9$ in a ceramic yield of 82.49 %.

Reaction of cerium acetate $Ce(O_2CCH_3)_3$ with molybdenum trioxide (MoO_3)

$Ce(CH_3COO)_3 1.6\ H_2O$ (6.140 g, 20 mmol) was dissolved in 100 ml of distilled water in a round flask. Molybdenum trioxide (MoO_3) was subsequently added to the result

solution. The mixture was then heated to reflux for one day. The pH at the beginning of the reaction was found to be 7.1 while at the end it was 4.3. The yellow product was isolated by filtration, washed with water, and then dried in a vacuum for 24 hours. The yield of the $Ce(O_2CCH_3)(MoO_4)\bullet 4H_2O$ was 3.506 g, or 91.23 % based on the amount of MoO_3 used.

RESULTS AND DISCUSSION

Reaction of MoO_3 with lanthanum acetate

A mixture of a stoichiometric amount of molybdenum trioxide and a solution of lanthanum acetate in water was heated at reflux for eleven days. During that time, lanthanum was absorbed from the solution to produce a white solid. The composition, $La(O_2CCH_3)(MoO_4)\bullet 1.05H_2O$ was determined from its thermal gravimetric analysis. The TGA trace, shown in (Figure 2.1.), had two weight loss steps. The first step occurred over the temperature range of 200 ℃ to 240 ℃ can be attributed to dehydration. This was confirmed by FTIR spectroscopy as discussed below. The weight loss for this step was 5.05 % corresponding to 1.05 equivalents of water. the second weight loss 13.93 %, occurred over the range of 460 ℃ to 480 ℃ and corresponded to the conversion of one equivalent of acetate to oxide. A strong exotherm indicated that this step involved combustion of the organic residues. The formula $La(O_2CCH_3)(MoO_4)\bullet 1.05H_2O$ was confirmed by carbon analysis by combustion. The calculated percent carbon for this formula is 6.39 % while the analytical result was 6.43 %.

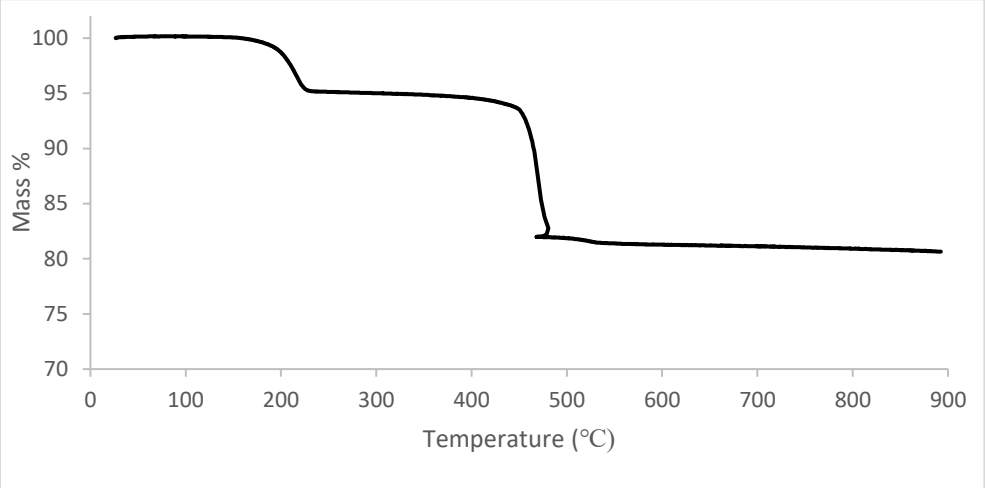

Figure 2.1. Thermal Gravimetric Analysis of $La(O_2CCH_3)(MoO_4)\bullet 1.05H_2O$

The infrared spectrum of lanthanum acetate is provided in (Figure 2.2) and that of $La(O_2CCH_3)(MoO_4)\bullet 1.05H_2O$ is shown in (Figure 2.3).

Both spectra show bands attributable to acetate groups in the range 1400 cm^{-1} to 1500 cm^{-1} that are due to the symmetric and asymmetric stretching vibrations of the CO_2 group of acetate confirming the presence of acetate in the product from the reaction of lanthanum acetate with MoO_3. The latter compound actually shows three absorption peaks of this type suggesting the presence of two different types of acetate groups. It also has strong bands at 849, 803, 787 cm^{-1}. These are analytical of a tetrahedral molybdate ion suggesting that molybdenum is present as an octahedral ion or polymeric or oligomeric species. There is also a small peak at 1649 cm^{-1} that can be attributed to the bending

vibration of a water molecule attached to a metal ion. The water stretching modes are not resolved in the spectrum, possibly due to being very broad and weak.

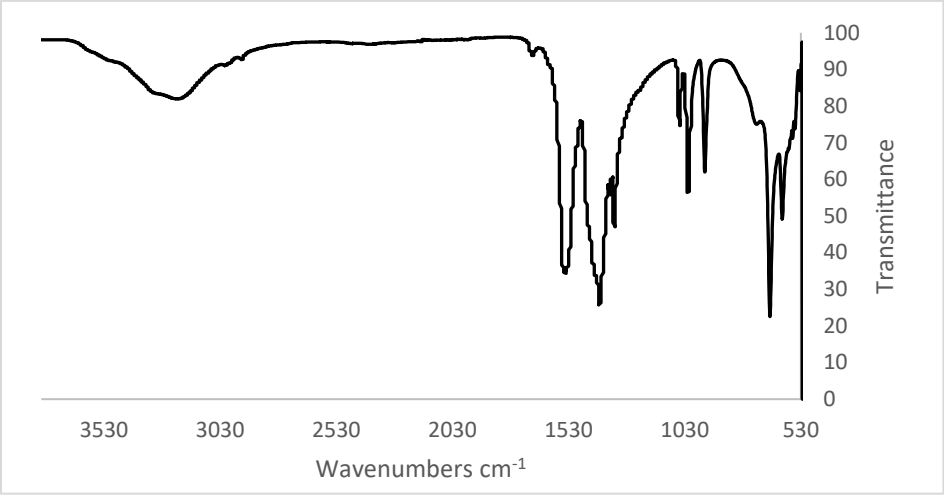

Figure 2.2. Infrared Spectrum of $La(O_2CCH_3)_3 \bullet 1.5H_2O$

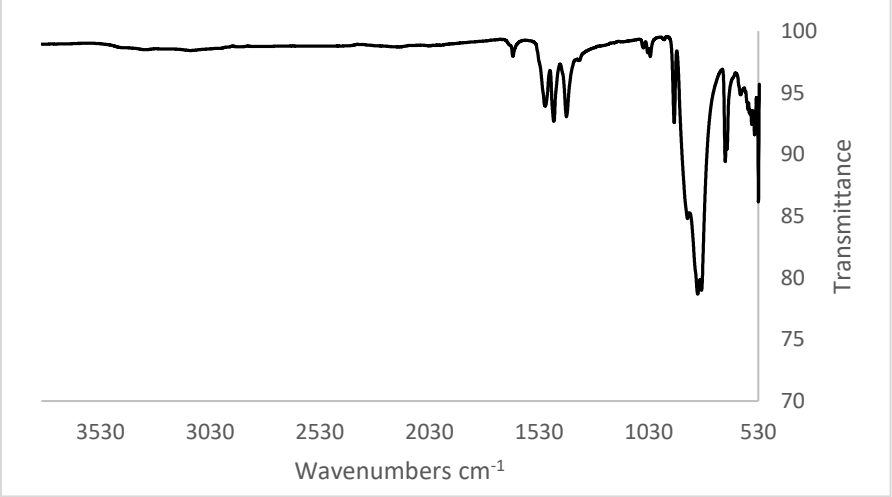

Figure 2.3. Infrared Spectrum of $La(O_2CCH_3)(MoO_4) \bullet 1.05H_2O$

The precursor was fired at two different temperatures at 300 ℃ and 500 ℃ in a muffle furnace. The infrared spectroscopy of the dehydrated product produced at 300 ℃ had peaks 1508, 1460, 1401 cm^{-1} at 300 ℃ (Figure 2.4) over the precursor converted into a bimetallic oxide $Ln_2Mo_2O_9$ after firing at 500 ℃. The infrared spectrum showed disappearance of the acetate groups and marked changes in the molybdenum oxygen vibrations. The narrower vibrations were replaced with a very broad unresolved peak that extended over the range from the 535 to 940 cm^{-1}.

These are not very different from those in the hydrated product (1502, 1463, and 1405 cm^{-1}) indicting that dehydration did not have a major effect on the coordination mode of acetate in the compounds. Dehydration did have a major effect on the Mo-O stretching frequencies. A new strong broad band was observed at 782 cm^{-1} and the higher wavenumber peaks in the hydrated compound disappeared. This suggests that the initial product from reaction of MoO_3 with lanthanum acetate contains molybdenum oxide moieties that can have bound water molecules. For example, The $MoO_5(OH_2)$ octahedra observed in transition metal hydrated molybdates. Notably, the peak at 1649 cm^{-1} for the H-O-H bending mode of metal- bound water disappears upon dehydration.

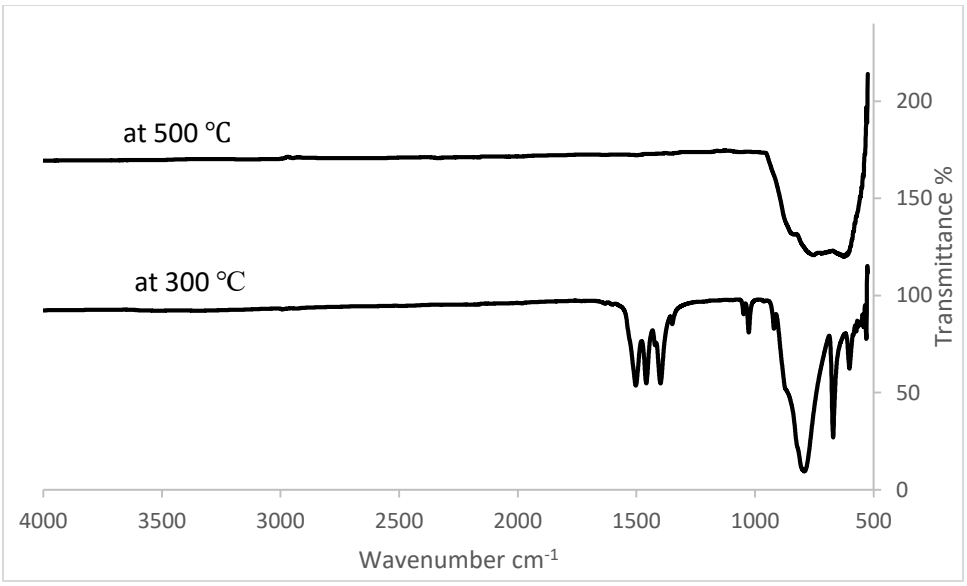

Figure 2.4. Infrared Spectra of products from firing $La(O_2CCH_3)(MoO_4)\bullet 1.05H_2O$ at 300 ℃ and 500 ℃

The X-ray powder diffraction pattern of the ceramic produced by heating the lanthanum molybdate acetate had an excellent match with the cubic phase of lanthanum molybdenum oxide ($Ln_2Mo_2O_9$) (Figure 2.6.). The as-prepared lanthanum acetate molybdate $La(O_2CCH_3)(MoO_4)\bullet 1.05H_2O$ was determined to be crystalline but the pattern did not match a known phase.

In agreement with the infrared spectrum, the solid-state carbon-13 NMR spectrum contained peaks for two different acetates **(**Figure 2.7). There were two peaks for carboxylate groups at 191 and 189 ppm and two peaks for methyl groups observed at 30 and 27 ppm. It is not possible to determine which pair of peaks are associated with each other of this time.

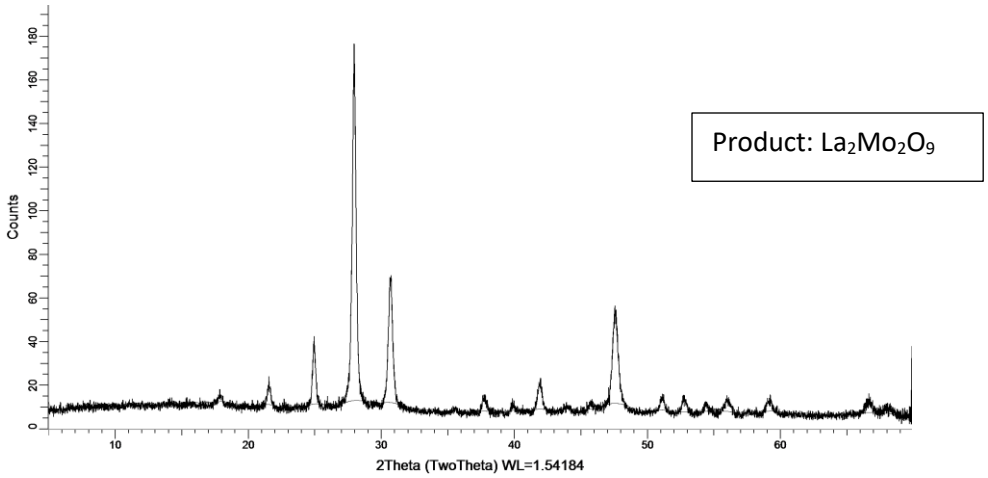

Figure 2.5. The XRD Pattern of the Product Ceramic Product by Heating $La(O_2CCH_3)(MoO_4)\bullet 1.05H_2O$ to 500 °C.

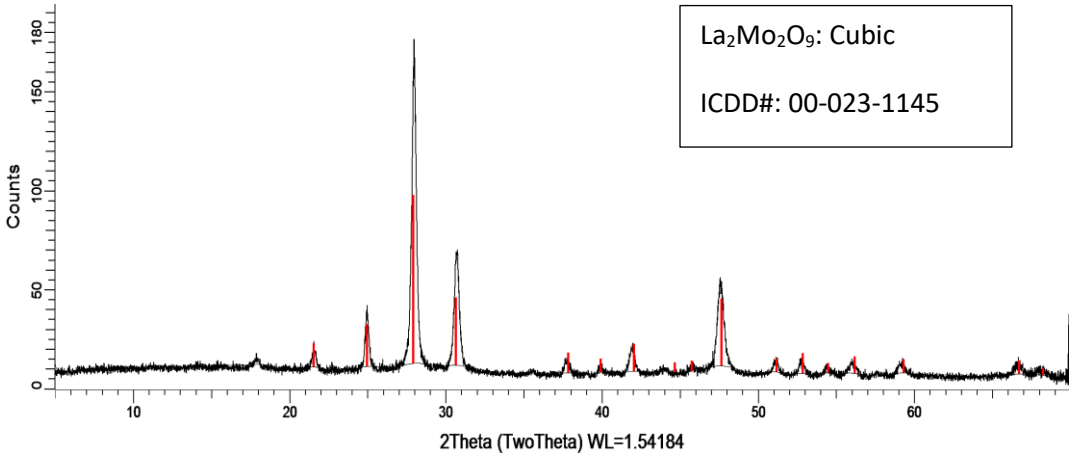

Figure 2.6. The XRD Pattern Match for Ceramic Product by Heating $La(O_2CCH_3)(MoO_4)\bullet 1.05H_2O$ to 500 °C.

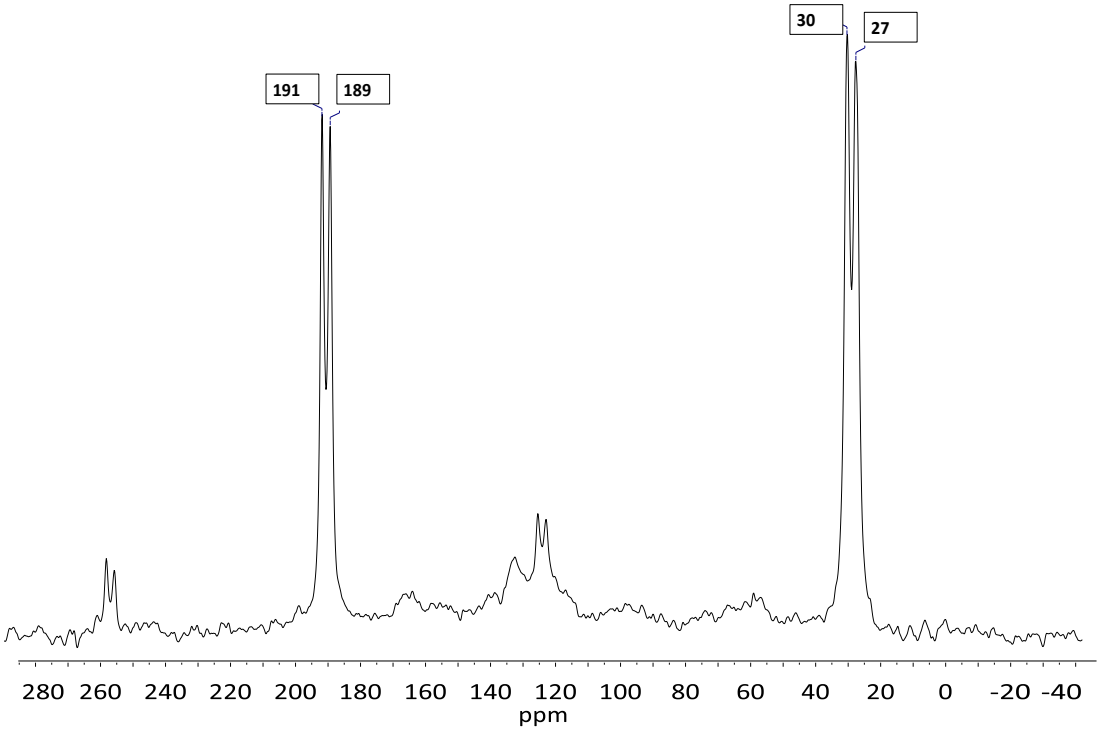

Figure 2.7. Carbon-13 NMR Spectrum of $La(O_2CCH_3)(MoO_4)\bullet 1.05H_2O$

In order to be able to make praseodymium doped $La_2Mo_2O_9$ is necessary to prepare the lanthanide molybdate acetate without using excess metal acetate. The excess acetate is used to buffer the reaction mixture. For example, the 2:1 lanthanum acetate:MoO_3 reaction had a pH of 4.5, close to the pka of acetic acid. When the reaction was performed with a 1:1 ratio of the reactants, the pH was 3.1. Infrared spectroscopy indicated that the product was the same as that from the 2:1 reaction. Therefore, the 1:1 reaction is a viable method for making the lanthanide molybdate acetate (Figure 2.8)

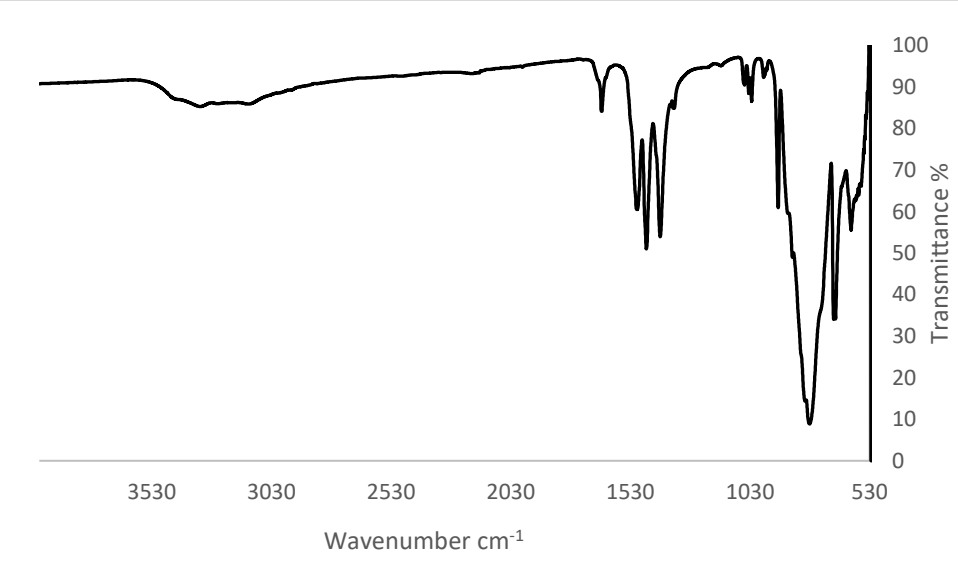

Figure 2.8. Infrared Spectra of the Product from Reaction of MoO_3 with one Molar Equivalent of Lanthanum Acetic

Kinetic of the Lanthanum Acetate/MoO_3 Reaction

Therefore, Microwave plasma-atomic emission spectroscopy (MP-AES) was used to follow the change of the concentration of lanthanum as lanthanum acetate reacted with MoO_3. Similar to reaction described above, $La(CH_3CO_2)_3 \bullet 1.5H_2O$ (7.138 g, 20 mmol) was dissolved in 100 ml of distilled water, and then molybdenum trioxide (MoO_3) was added. The reaction was then refluxed for eight days while, 80 microliters (0.08 g) of the samples were collected approximately every twenty four hours. After that, all samples were diluted by 250 ml of distilled water and the lanthanum concentrations were determined by MP-AES (microwave plasma atomic emission spectroscopy). Interestingly, the reaction reached completion in the first day of the reaction (Table2.1). Since a one-fold excess of

lanthanum acetate was used, the reaction ended when the concentration of lanthanum had dropped 50 %. This approaches to have occurred at some point in the first 25 hours.

Table2.1. Concentration of lanthanum (ppm) Versus Time for an 8-Day reaction

Time (Hours)	Concentration of lanthanum (ppm)	Time (Hour)	Concentration of lanthanum (ppm)
0	$2.65*10^4$	90.9	$1.29*10^4$
0.5	$2.26*10^4$	116.9	$1.29*10^4$
25.3	$1.29*10^4$	137.9	$1.33*10^4$
44.9	$1.28*10^4$	162.9	$1.35*10^4$
68.9	$1.31*10^4$	186.9	$1.35*10^4$

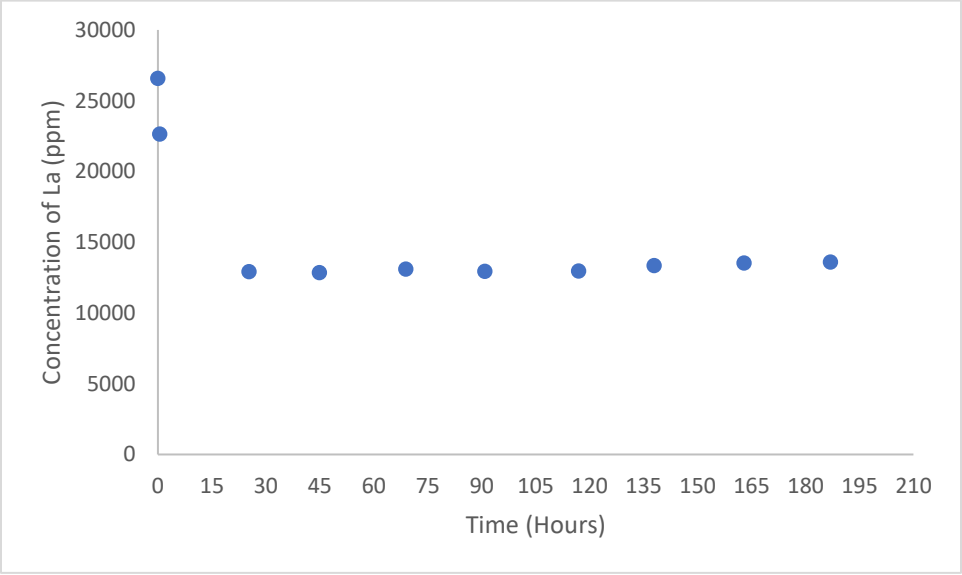

Figure 2.9. Concentration of Lanthanum Versus Time During the Reaction of Lanthanum Acetate with MoO_3

The experiment was reported over an 8-hour period with sampling every hour. This gave the data tabulated in (Table 2.2) and shown graphically in (Figure2.10).

The lanthanum concentration data was analyzed and it was found the reaction of lanthanum acetate with MoO_3 had a first order dependence on La^{3+}. The calculated rate constant was 0.32 hr^{-1}. This value was quite similar to that of the uranyl ion with MoO_3 that had a value of 0.34 hr^{-1} under similar conditions.

Table 2.2. Concentration of Lanthanum Versus Time for Reaction of Lanthanum Acetate with MoO_3 over an 8-Hour Time Period

Time (Hour)	Concentration of La (ppm)	Time (Hour)	Concentration of La (ppm)
0	$2.44*10^4$	4	$2.27*10^4$
1	$2.37*10^4$	6	$2.25*10^4$
2	$2.31*10^4$	7	$2.23*10^4$
3	$2.29*10^4$	8	$2.23*10^4$

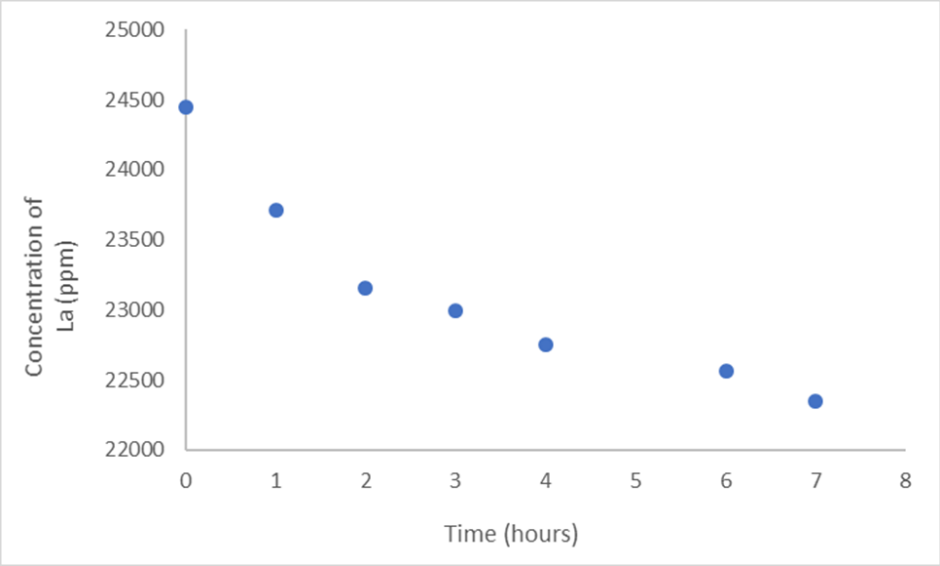

Figure 2.10. Plot of Concentration of Lanthanum Versus Time for Reaction of Lanthanum Acetate with MoO_3 over an 8-Hour Time Period

Reaction of Cerium acetate with MoO_3

The reaction of cerium acetate with MoO_3 proceeded in the same manner as that of lanthanum acetate. A drop in pH from 7.0 to 4.3 occurred as the reaction proceed acetic acid and reached the buffer point of the acetic acid/acetate system. Unlike the white lanthanum product, the cerium product was a light-yellow color. X-ray powder diffraction showed that both products are isostructural. The individual patterns are shown in patterns for lanthanum molybdate acetate and cerium molybdate acetate respectively (Figure 2.11) and (Figure 2.12).

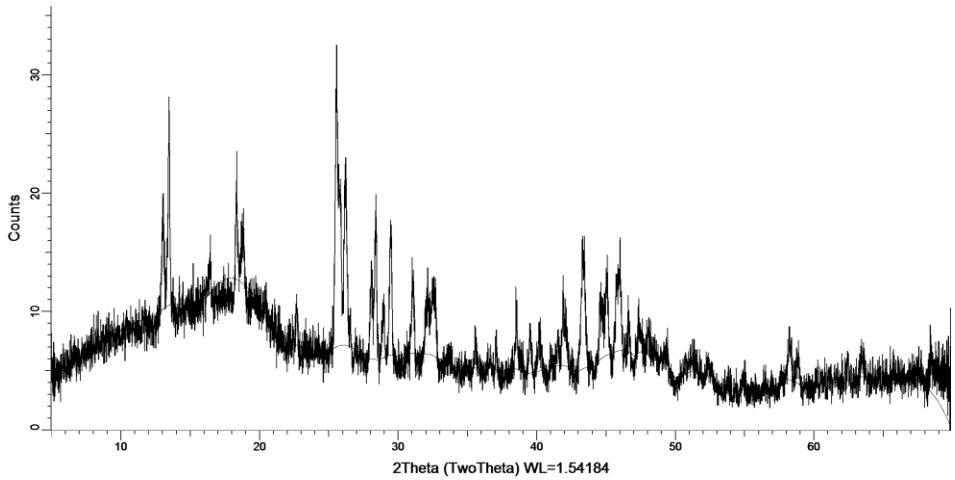

Figure 2.11. The XRD Pattern of Lanthanum Molybdate Acetate

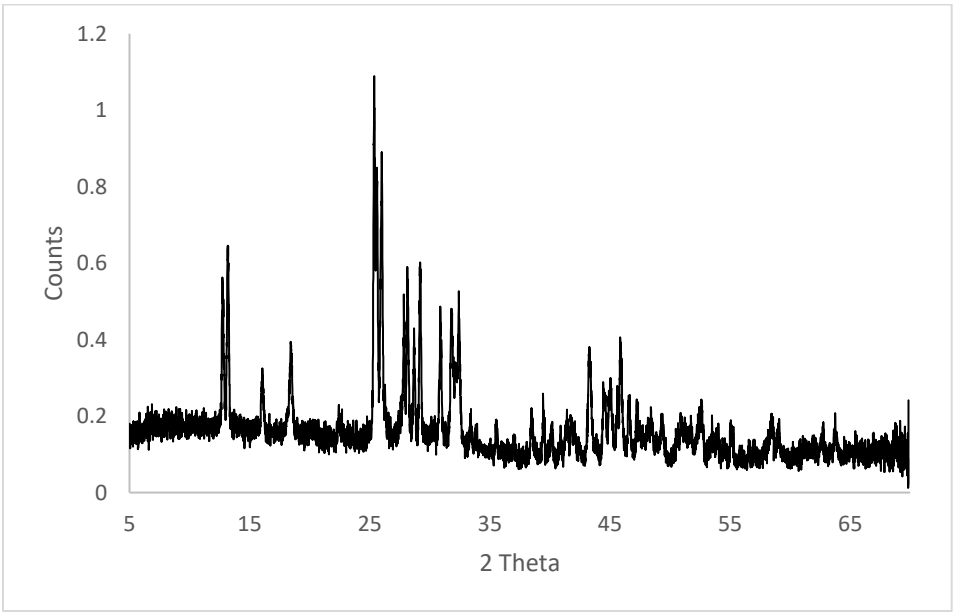

Figure 2.12. The XRD Pattern of Cerium Molybdate Acetate

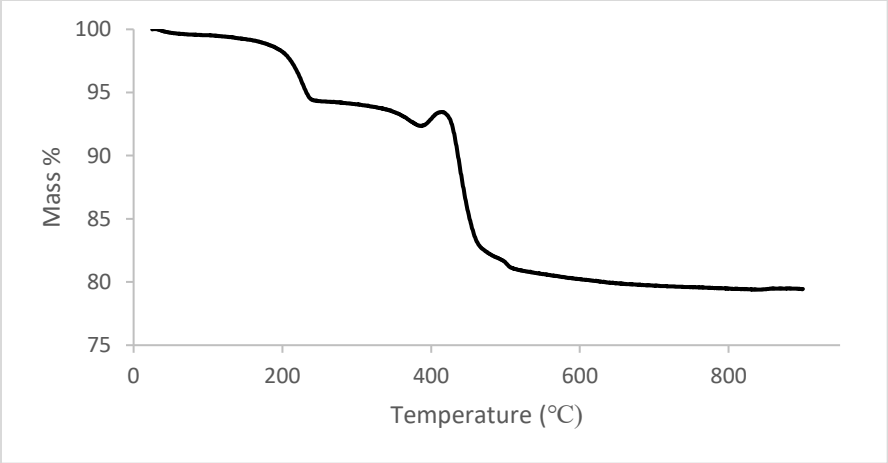

Figure 2.13. Thermal Gravimetric Analysis of the Product from the Reaction of Cerium Acetate with MoO_3

The thermal gravimetric analysis trace for the cerium molybdate acetate is shown in (Figure 2.13). An initial weight loss of loosely bound water was observed between 29 ℃ and 71 ℃. The change was 1.4 % and corresponded to loss of 0.30 equivalents of water. Tightly bound water was lost over the range 105 ℃ to 252 ℃ giving a mass loss of 5.2 % due to release of 1.10 equivalents of water. The weight change as acetate is removed is complicated by overlap with a weight gain due to oxidation of cerium (III) to cerium (IV). Acetate removal began at 252 ℃ and as this decomposition progressed, cerium (III) was destabilized and reached with oxygen carbon dioxide to form $[Ce_2(CO_3)]^{4+}$. This transformation is calculated to cause a weight gain of 0.78 % while the actual change was found to be a gain of 0.79 % over the temperature range 380 % to 409 %. The decomposition of acetate and carbonate continued up to 475 % when the ceramic yield was 82.3%, corresponding to $CeMoO_5$. $CeMoO_5$ has been observed in the gas phase above a melt of cerium molybdate but it has never been reported as a solid phase. As the temperature increased to 822 ℃, a gradual weight loss of 2.8 % that can be attributed to

conversion of $CeMoO_5$ to $Ce_2Mo_2O_9$ as oxygen evolved white Ce (IV) was reduced to Ce (III). The thermal gravimetric analysis results are consistent with a formula of $Ce(MoO_4)(O_2CCH_3)\bullet 1.4H_2O$ for the product isolated from reaction of MoO_3 with cerium acetate. This formula was also supported by elemental analysis for carbon: that calculated for the above formula 6.25 % and that found was 6.24 %.

The infrared spectrum of cerium acetate molybdate (Figure 2.14) was very similar to that of lanthanum molybdate acetate. It had an intense peak due to a stretching vibration of molybdenum oxide 781 cm^{-1}, and three peaks at 1401, 1462, 1404 cm^{-1} due to C-O stretching vibrations of acetate. Furthermore, when the product was dried at 250 ℃, it produced a material with an infrared spectrum (Figure 2.15) identical to that of the dried lanthanum acetate molybdate.

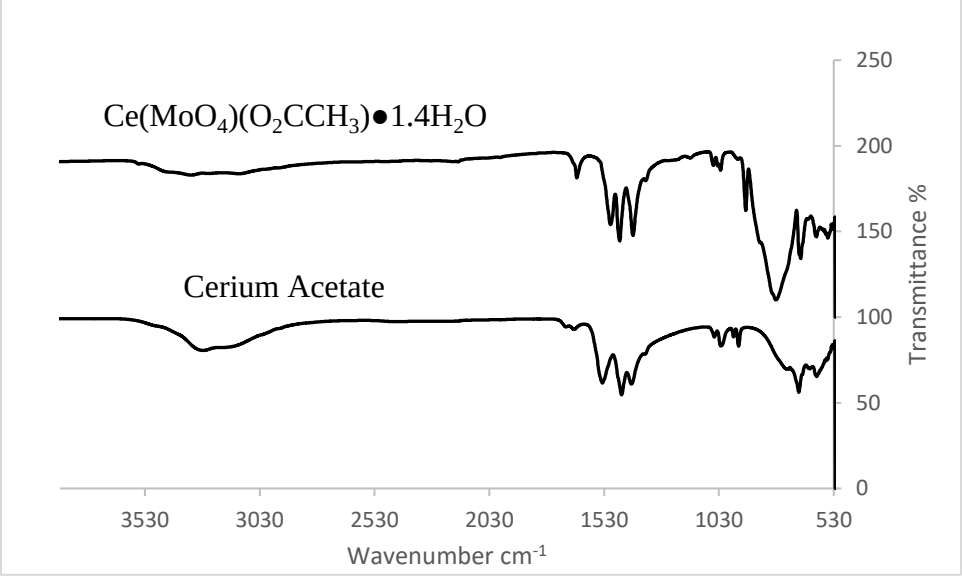

Figure 2.14. A Comparison of the Infrared Spectra of Cerium Acetate and $Ce(MoO_4)(O_2CCH_3)\bullet 1.4H_2O$

.

Figure 2.15. The Infrared of Dehydrated $Ce(MoO_4)(O_2CCH_3)\bullet 1.4H_2O$

Conclusions

The reaction of cerium acetate and lanthanum acetate both produce lanthanide acetate molybdates. This defines the range of lanthanide ionic radii formation of acetate as 1.032 Å to 1.010 Å. These materials are useful precursors for $Ln_2Mo_2O_9$, materials with useful ionic conductivity and catalytic and optical properties.

CHAPTER III

SYNTHESIS OF YTTRUIM AND PRASEODYMIUM HYDROXIDE MOLYBDATES AND PRASEODYMIUM/LANTHANUM ACETATE MOLYBDATES

Introduction

Mixed-metal oxides play a remarkable role in many chemical fields, physics, and materials science[53]. The combination of two metals in an oxide compound can produce materials with superior performance in industrial applications[54]. Pure yttrium oxide, for example, can be doped with a variety of metals for use several applications. For example, Y_2O_3:Eu is important that can be used in plasma display panels and fluorescent lamps. Also, several methods have been reported in literature to prepare yttrium oxide from solid-state decomposition reactions[55]. In this research, praseodymium was doped into lanthanum molybdate acetate, $La(O_2CCH_3)(MoO_4)\bullet XH_2O$ and fluorescence spectroscopy was used to investigate luminescence of the $La_2Mo_2O_9$:Pr prepared from it. Raman spectroscopy was used to follow structural changes before and after doping.

Experimental

Reaction of yttrium acetate $Y(O_2CCH_3)_3$ with molybdenum trioxide (MoO_3)

Another metal acetate that was chosen based on its ionic radius was a transition-metal. Yttrium is located just above lanthanide in the periodic table. MoO_3 (1.44 g, 10 mmol) was allowed to react with a solution of yttrium acetate tetrahydrate (6.89 g, 20 mmol) in 100 ml of water at reflux for a week. Upon cooling, the solid was isolated at room temperature by filtration through a fine sintered glass filter. The yield was 2.84 g (100 %) of Y(MoO4)(OH)•H_2O. Product was characterized by the thermal gravimetric analysis (TGA) and inferred spectroscopy.

Reaction of praseodymium acetate $Pr(CH_3COOH)_3$ hydrate with molybdenum trioxide (MoO_3)

MoO_3 (1.446 g, 10 mmol) was added to a solution of praseodymium acetate (6.29 g, 20 mmol) in 100 ml of water and the mixture was heated to reflux for six days. The product was isolated by filtration and was dried in vacuum in room temperature for two days to give a yield of 3.01 g (89.5 %) of $Pr(MoO_4)(OH)•H_2O$. The product was characterized by inferred spectroscopy and the thermal gravimetric analysis.

Reaction of molybdenum trioxide with lanthanum acetate and praseodymium acetate mixture.

MoO_3 (1.44g, 10 mmol) was reacted with a solution of lanthanum acetate (3.06 g, 0.9 mmol) and praseodymium acetate (0.333, 1.0 mmol) in 100 ml of the distilled water at reflux for a week. the resulting white solid was isolated by filtration and vacuum-dried at room temperature for one day. The yield $La_{0.9}Pr_{0.1}(O_2CCH_3)_2(MoO_4)\bullet H_2O$ was 3.547 g (94.1 %).

The reaction was reported with equivalent amounts of the lanthanide were made in order to test the amount of praseodymium that can be included and to still form acetate molybdate phase. Therefore, a solution of lanthanum acetate (1.695 g, 5.0 mmol and praseodymium acetate (1.666 g, 5.0 mmol) were dissolved in 100 ml of the distilled water was prepared. Upon cooling, the product was isolated by filtration and dried in vacuum at room temperature overnight. The weight of the product was 3.473 g. Next, 1.43 g (10 mmol) of MoO_3 was added to this solution and the mixture was refluxed for one week. The product was isolated by filtration and dried in a vacuum over ambient temperature overnight. The yield of $La_{0.5}Pr_{0.5}(O_2CCH_3)_2(MoO_4)\bullet H_2O$ was 3.473 g (92.1 %) all these products were run in Raman spectroscopy.

RESULTS AND DISCUSSION

Reaction of molybdenum trioxide with yttrium acetate

An extremely sharp peak was observed at 3569 cm^{-1} in the infrared spectroscopy of $Y(MoO_4)(OH)•H_2O$ that corresponds to a stretching vibration of O-H and the sharpness implies that there is no H-bonding (Figure 3.1). Unlike, the lanthanum and cerium products, the product contained very little acetate. There were weak peaks of 1546 cm^{-1} and 1400 cm^{-1} that likely due to traces of acetate at the surface of the yttrium product. Analysis for carbon gave a result of 0.43 % or only 0.02 per yttrium.

In the range where molybdenum oxygen stretches are expected, there are a series of sharp bands at 943, 913, and 823 cm^{-1} and an intense broader bond at 704 cm^{-1} with a shoulder at 638 cm^{-1}. This is very similar to the infrared spectrum reported by the Apblett research group for cobalt molybdate hydrate [3]. There an almost identical pattern of peaks was observed at 960, 913, 817, and 725 cm^{-1}. Cobalt molybdate has a structure that contains a cluster of two cobalt $CoO_5(OH_2)$ and two MoO_4 tetrahedra shown in (Figure 3.2)[56]. If the Co^{2+} ions were reported by $[Y(OH)]^{2+}$ ions, a similar cluster could be produced. Further research is required to confirm this proposed structure.

Figure 3.1. Infrared Spectrum of $Y(MoO_4)(OH)\bullet H_2O$

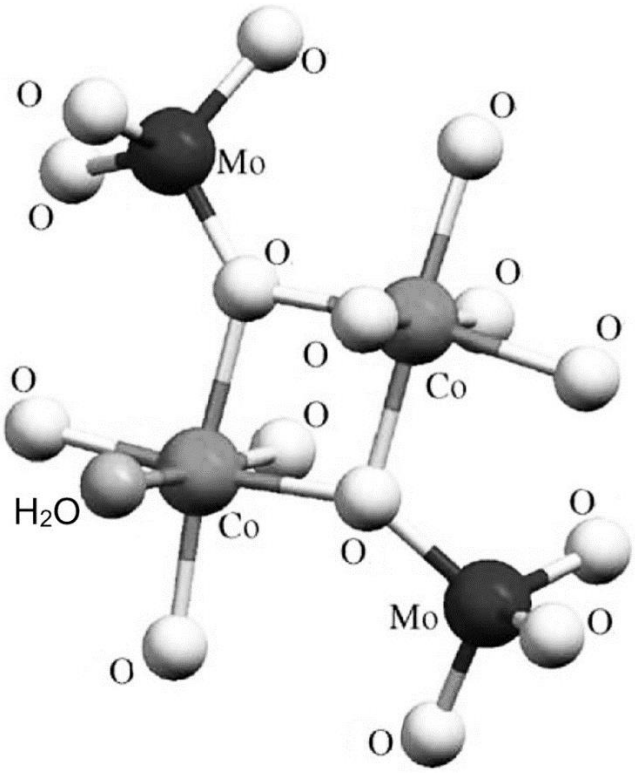

Figure 3.2. Metal Oxide Cluster Present in $CoMoO_4\bullet H_2O$ (Taken from[3]).

Figure 3.3 shows the TGA trace for the yttrium acetate/MoO_3 produced. The dehydration of $Y(MoO_4)(OH)\bullet H_2O$ was also similar to that of $CoMoO_4\bullet H_2O$[3]. Loosely bound water lost at lower temperature while the last half equivalent of water required temperatures above 350 ℃. The higher weight loss step as observed in (Figure 3.3) is likely due to loss of the hydroxide groups as water. Note that the mass continues to fall slowly up to 900 ℃. This is the hallmark of a solid in which hydroxides must diffuse in order to combine to form water and oxide ions.

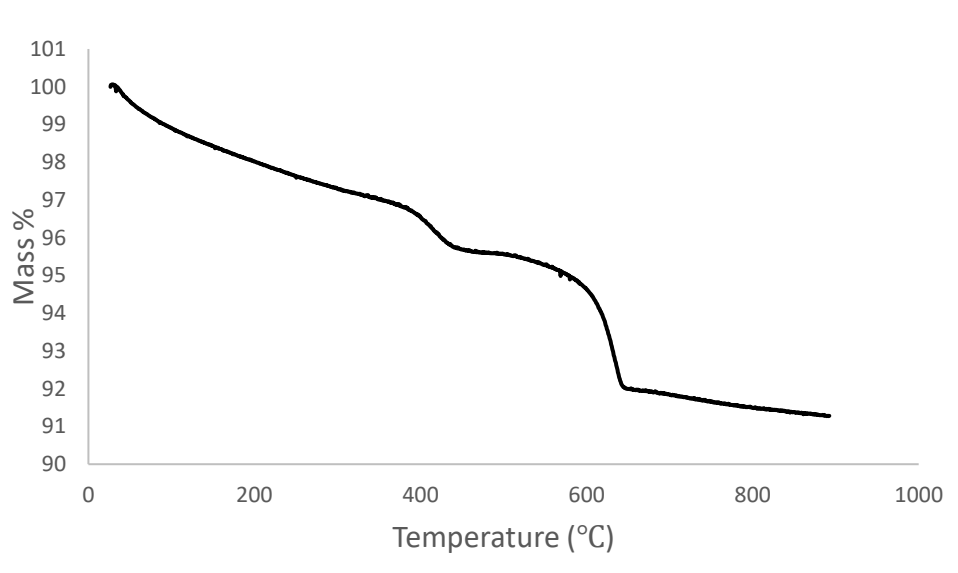

Figure 3.3. Thermal gravimetric analysis of $Y(MoO_4)(OH)\bullet H_2O$

Reaction of MoO_3 with praseodymium acetate

The reaction of MoO_3 with praseodymium acetate produced $Pr(MoO_4)(OH)\bullet H_2O$ that had an infrared spectrum almost identical to the yttrium acetate/MoO_3 product (Figure

3.4). Again, traces of acetate were present and elemental analysis showed 0.42 % carbon or about 0.023 molar equivalents per praseodymium.

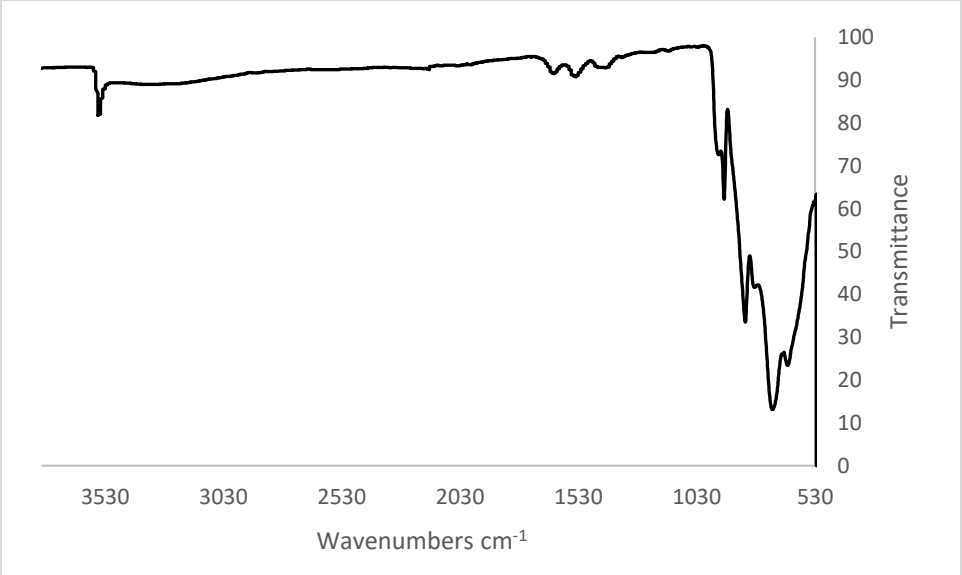

Figure 3.4. Infrared spectrum of $Pr(MoO_4)(OH)•H_2O$

Thermal gravimetric analysis of $Pr(MoO_4)(OH)•H_2O$ also showed similar series of weight losses (Figure 3.5) as those observed for the yttrium analogue. The similarities in the thermal analysis and the infrared spectra suggest that the yttrium and praseodymium molybdate hydroxides are isostructural. These compounds should also serve as precursors for $Ln_2Mo_2O_9$ (Ln = Y, Pr) but higher temperatures will be required for synthesis of the oxides due to difficult and slow dehydroxylation. However, the slow loss of water at high temperature suggests the possibility of production of active catalyst materials in the same way that dehydration of $Al(OH)_3$ produces activated alumina.

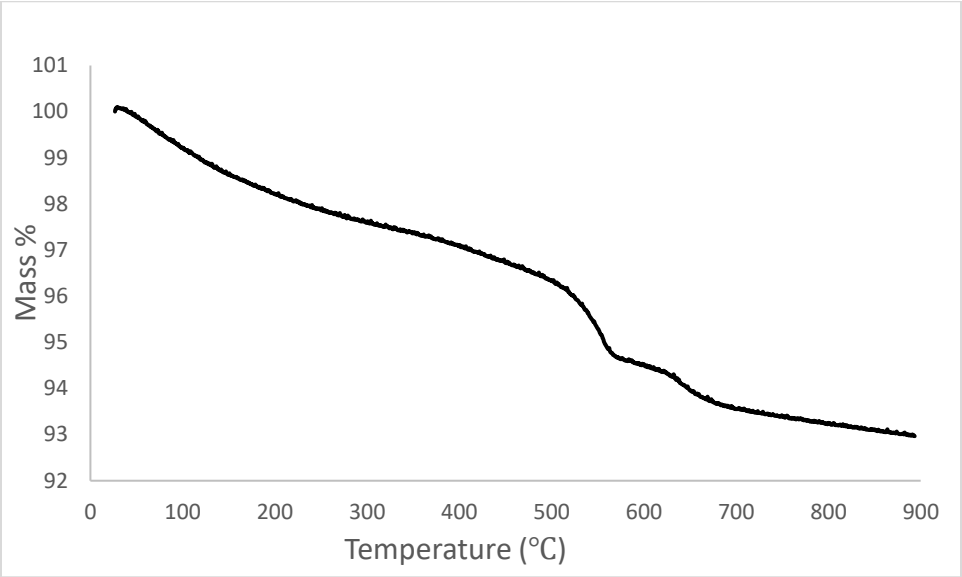

Figure 3.5. Thermal gravimetric analysis of the product from praseodymium acetate with MoO_3.

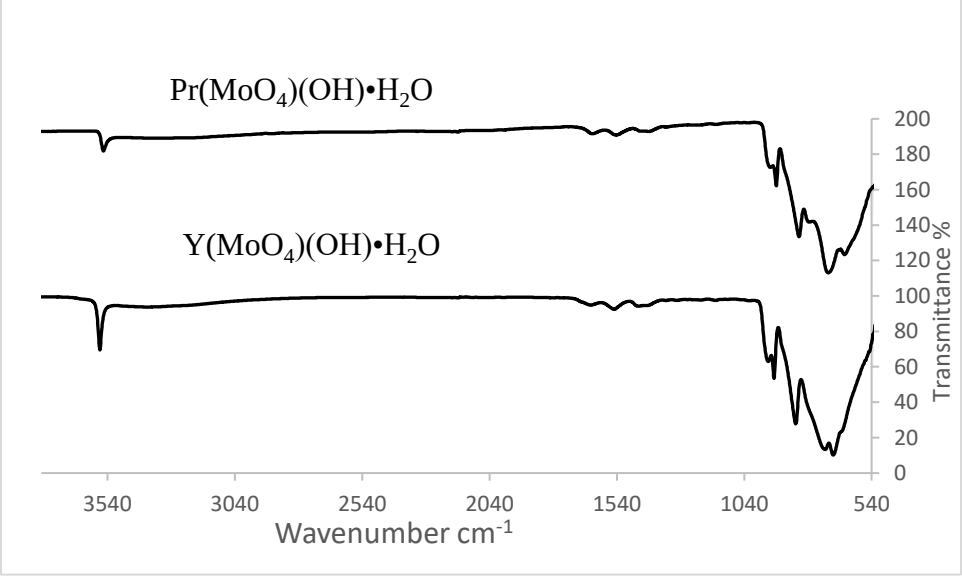

Figure 3.6. A comparison of the Infrared spectra of $Y(MoO_4)(OH)•H_2O$ and $Pr(MoO_4)(OH)•H_2O$

Preparation of $La_2Mo_2O_9:Pr^{3+}$ phosphors and Related Compounds

$La_2Mo_2O_9$ has two phases, a high-temperature forms β-$La_2Mo_2O_9$ is cubic and a low-temperature forms α-$La_2Mo_2O_9$. The first type is an oxide ion conductor. On the other hand, β-$La_2Mo_2O_9$ has satisfactory chemical and thermodynamic stability for use as a host for phosphors. Ions can be doped either into the lanthanum site or the molybdenum site. Therefore, this allows the selection of appropriate ion doping compositions to enhance the luminescence of the system[4]. Previously, praseodymium was doped into β-$La_2Mo_2O_9$. A series of phosphors $La_{2x}Pr_xMo_2O_9$ (x=0.01–0.10) were prepared by solid state reaction at high temperature (800 – 900 ℃). Finally, samples were cooled to room temperature for characterization purposes. All samples produced a red emission peak at 650 nm under excitation by 450 nm blue light. As shown in (Figure 3.7) increasing Pr content (x) increases the emission intensity up to the optimal amount where x = 0.07. Three sharp lines were observed of 604 nm, 620 nm, and 650 nm (Figure 3.8).[4]

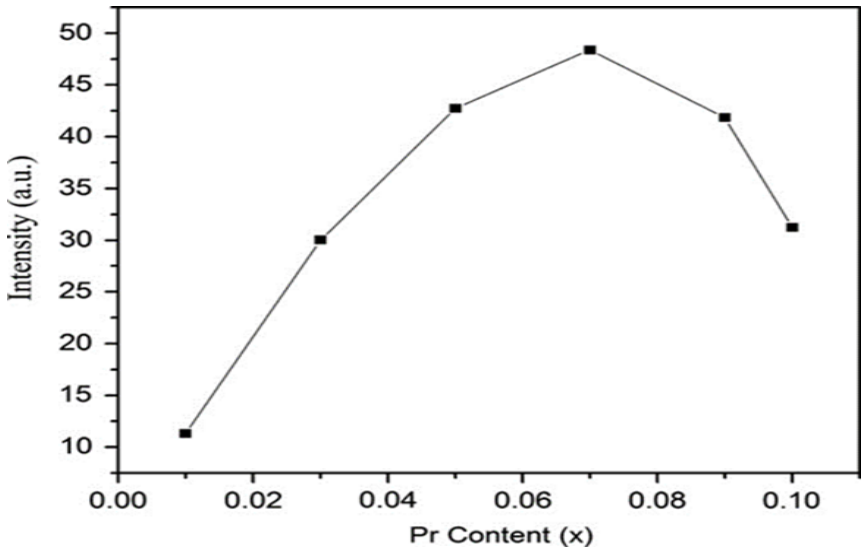

Figure 3.7. Dependence of the emission intensity on praseodymium content of $La_{2-x}Pr_xMo_2O_9$ as reported by Zhang and co-workers.[4]

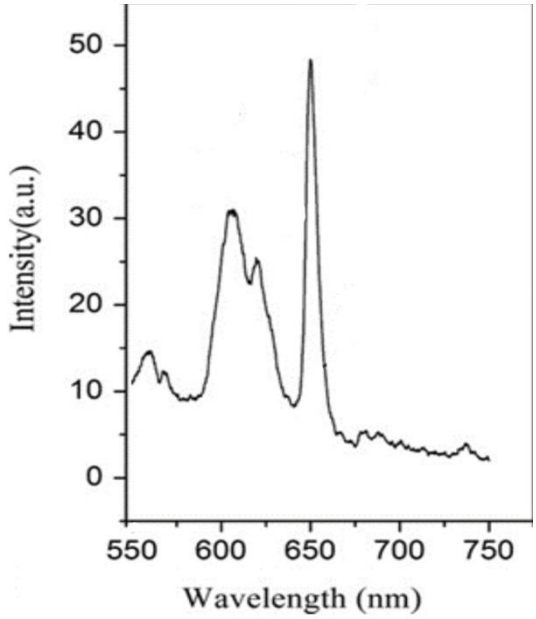

Figure 3.8 Emission spectra of $La_{1.93}Pr_{0.07}Mo_2O_9$ prepared by a solid-state reaction at 900 °C. The excitation wavelength was 450 nm. The figure was adapted from that reported by Zhang and co-authors.[4]

As discussed in chapter 1, reactions of molybdenum trioxide with lanthanide acetate were found to generate a lanthanide molybdate acetate. The thermal gravimetric analysis (Figure 3.9) for $La_{0.9}Pr_{0.1}(CO_2CH_3)_2(MoO_4)\bullet H_2O$ was almost identical to that of pure lanthanum compound, shown a 4.15 % weight loss due to dehydration followed by a 13.24 % loss as acetate decomposed to oxide.

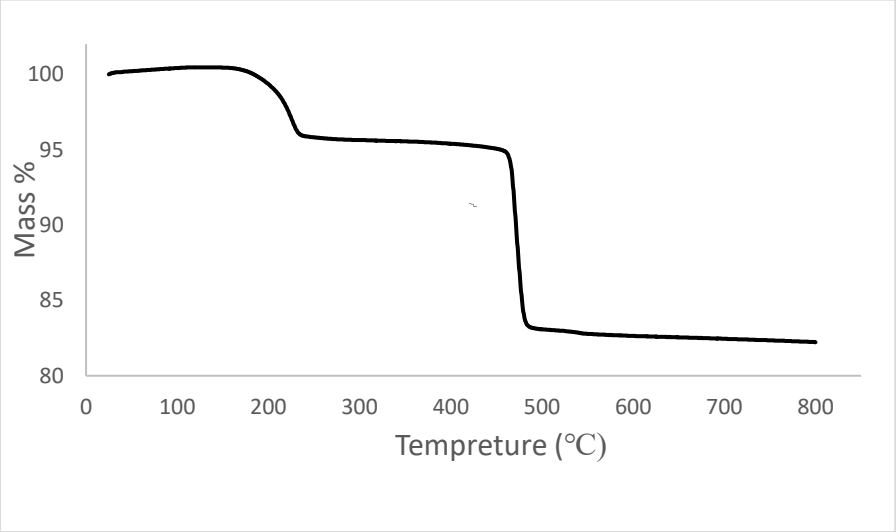

Figure 3.9. Thermal gravimetric analysis of $La_{0.9}Pr_{0.1}(O_2CCH_3)(MoO_4)\bullet H_2O$

Figure 3.10 and Figure 3.11 show the Raman spectra for $La_{1-x}Pr_x(O_2CCH_3)(MoO_4)\bullet H_2O$ with x = 0.1 and 0.5, respectively. The spectra are almost identical showing, that even after with replacement of half of the lanthanum with praseodymium, only the molybdate acetate is formed and not the molybdate hydroxide. Both show C-O stretching frequencies for acetate at 1314 cm^{-1}. However, a third peak for the symmetric stretching mode is at 1357 cm^{-1} for x = 0.1 and 1348 cm^{-1}. This may indicate that at least one type of acetate group is bound to the lanthanide when there is more of the heavier lanthanide the band shifts to lower energy due to an increase in the reduced mass. The most prominent

feature of the spectra is an insert peak at 914 cm^{-1} for an M-O stretching mode. Other peaks in the region for M-O stretches are seen at 968, 823, 819 and 781 for both the low and high praseodymium content samples. Both compounds also have common peak for O-H stretching at 2918 cm^{-1} and low-frequency bands at 324 and 142 cm^{-1}.

Notably, the praseodymium molybdate hydroxide shows very similar peaks in the molybdenum-oxide stretching region as the molybdenum acetate compounds. The three most intense bands observed at 910, 823, and 783 cm^{-1} are within the instrument resolution of 914, 823, and 781 cm^{-1} observed for the acetate molybdate. Furthermore, the two most intense peaks are also very similar to the peaks for $CoMoO_4 \bullet H_2O$ observed at 918 and 821 cm^{-1}.[56]

Earlier in this chapter, the similarity of the infrared spectra of the lanthanide molybdate hydroxides of hydrated cobalt molybdate was commented on. The combination of both Raman and infrared spectroscopy strongly suggests that the hypothesis that the lanthanide and cobalt compounds have similar metal oxide building blocks has merit. It also appears that the lanthanide molybdate acetates also have a similar metal oxide cluster. The weaker Mo-O peaks vary from each other, 968 vs 933 cm^{-1}, and 810 vs 783 cm^{-1} for the acetate and hydroxide compounds, respectively. As expected, the low frequency region where lanthanide oxygen stretching vibrations are observed is quite different since acetate-metal stretches are different from hydroxide-metal stretches.

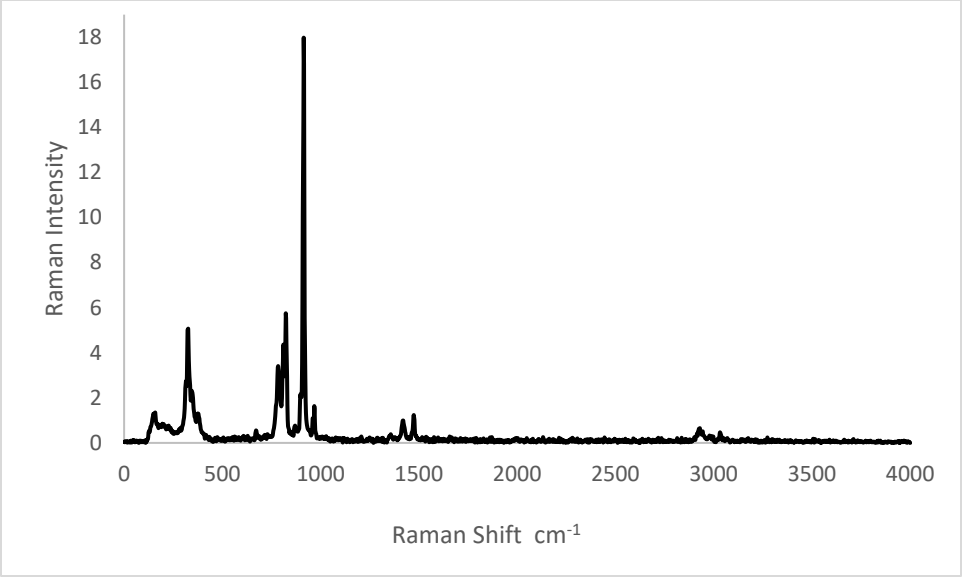

Figure 3.10. Raman Spectrum for $La_{0.9}Pr_{0.1}(O_2CCH_3)(MoO_4)\bullet H_2O$

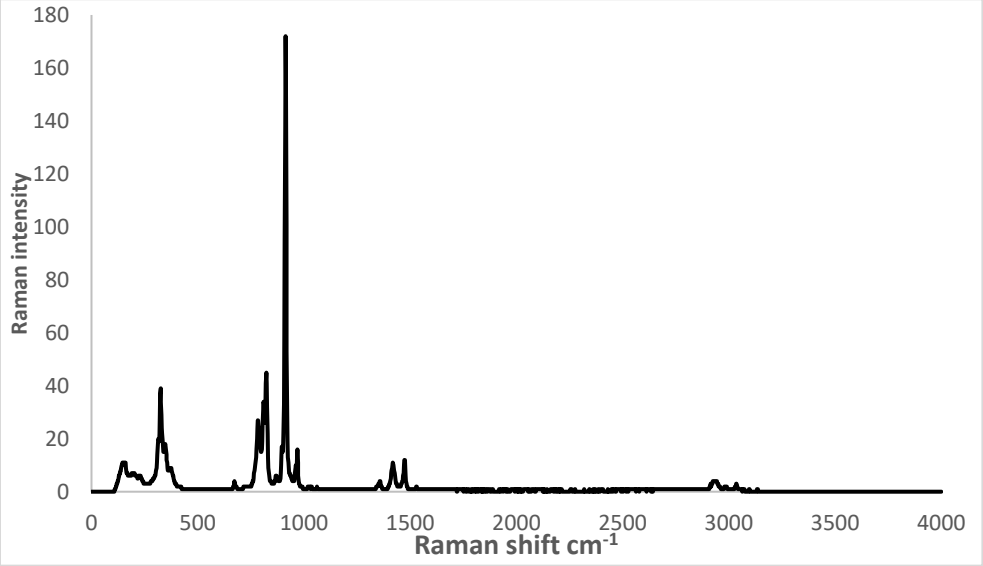

Figure 3.11. Raman Spectrum of $La_{0.5}Pr_{0.5}(O_2CCH_3)(MoO_4)\bullet H_2O$

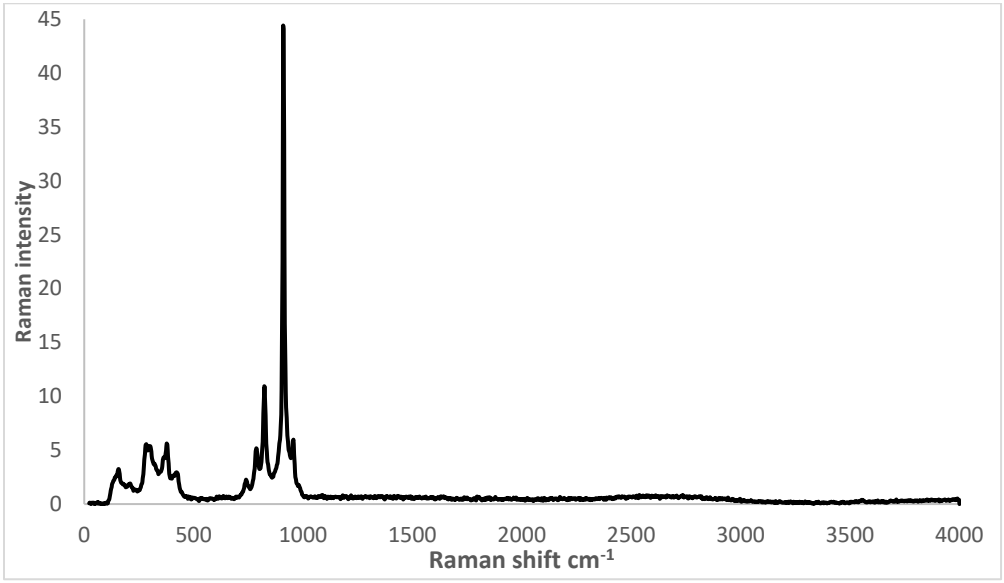

Figure 3.12. Raman Spectrum of $Pr(OH)(MoO_4)•H_2O$

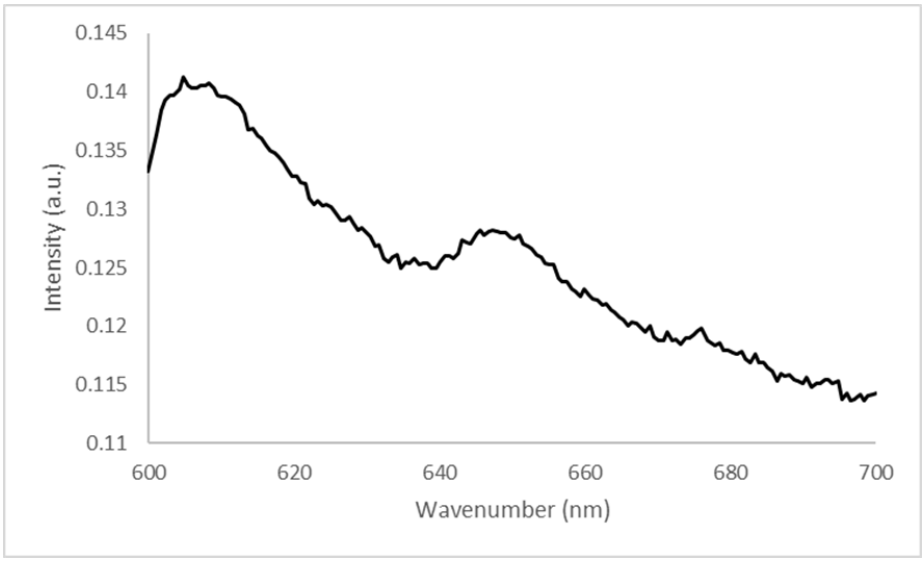

Figure 3.13. Emission Spectra of $La_{1.8}Pr_{0.2}Mo_2O_9$

A sample of 10 % praseodymium doped lanthanum molybdate acetate was fired at 800 °C to convert it to $La_{1.8}Pr_{0.2}Mo_2O_9$. The solid-state fluorescence was measured on a Cary Eclipse spectrometer using 450 nm excitation. Two emission peaks at 610 and 650 nm were observed in accordance with previous data reported for $La_2Mo_2O_9:Pr^4$. In this study, the peaks are broad because a weak light source and a difficult to align solid state stage made it necessary to use wide slits on the fluorimeter. The emission peaks are similar to those reported by Zhang and co-workers at 604 nm, 620 nm, and 650 nm if (Figure 3.18) if the first two peaks are unresolved. However, the intensities are reversed with 650 nm being the weaker emission band in this study. Thus, it must be concluded that this data is only preliminary and the fluorescence investigation will need to be repeated with an instrument that is more capable of measuring the fluorescence of solid-state compounds.

Conclusions

The ionic radius range in which the reaction of trivalent metal acetates with molybdenum trioxide will produce a metal acetate molybdate has that been defined. Y^{3+} (0.900 Å) and Pr^{3+} (0.990 Å) appear to be too small and instead form a molybdate hydroxide phase. On the other hand, La^{3+} (1.032 Å) and Ce^{3+} (1.010 Å) form the acetate phase readily. Unfortunately, it is not possible to test large trivalent metal ions since those available are either extremely air sensitive, radioactive, or both.

Both the molybdate hydroxide and the molybdate acetate phases appear to have a common lanthanide molybdenum oxide core base on similarities in vibrational spectroscopy. Further, that cluster may be similar to that found in $CoMo_4•H_2O$.

Interestingly, the presence of lanthanum appears allow praseodymium to also form the lanthanide molybdate acetate with up to 50 % praseodymium and probably beyond. This suggests layered compound where the presence of lanthanum acetate mortise open the interlayer gap leading to coordination of praseodymium by acetate as well. Otherwise, praseodymium (and acetate) presumably prefers acetate because it is smaller size makes binding of the smaller hydroxide ion more favorably. Both the lanthanide molybdate hydroxides and the lanthanide molybdate acetates are excellent precursors for stoichiometric $Ln_2Mo_2O_9$, materials that have several useful applications.

REFERENCES

1. Chippindale, A. M.; Cheetham, A. K., Chapter 3 - The Oxide Chemistry of Molybdenum. In *Studies in Inorganic Chemistry*, Braithwaite, E. R.; Haber, J., Eds. Elsevier: 1994; Vol. 19, pp 146-184.
2. Andersson, G.; Magneli, A., Crystal structure of molybdenum trioxide. *Acta Chem. Scand.* **1950,** *4*, 793-7.
3. Alqahtani, F. bimetallic single-source precursor appoach for synthesis of molybdenum-containing ternary oxides Oklahoma State University

Stillwater, 2018.
4. Zhang, D.; Shi, S.; Luo, M.; Zhou, J., Solid state reaction preparation and enhanced red luminescence of S-doped La2Mo2O9: Pr3+ phosphors. *Ceramics International* **2013,** *39* (6), 6299-6302.
5. Braithwaite, E. R.; Haber, J., *Molybdenum: an outline of its chemistry and uses*. Elsevier: 2013; Vol. 19.
6. Alves de Castro, I.; Datta, R. S.; Ou, J. Z.; Castellanos-Gomez, A.; Sriram, S.; Daeneke, T.; Kalantar-zadeh, K., Molybdenum Oxides - From Fundamentals to Functionality. *Adv. Mater. (Weinheim, Ger.)* **2017,** *29* (40), n/a.
7. Bagheri, S.; Muhd Julkapli, N., Mo3VOx catalyst in biomass conversion: A review in structural evolution and reaction pathways. *Int. J. Hydrogen Energy* **2017,** *42* (4), 2116-2126.
8. Cronin, L.; Kogerler, P.; Muller, A., Controlling growth of novel solid-state materials via discrete molybdenum-oxide-based building blocks as synthons. *J. Solid State Chem.* **2000,** *152* (1), 57-67.
9. de, C. I. A.; Datta, R. S.; Ou, J. Z.; Sriram, S.; Daeneke, T.; Kalantar-Zadeh, K.; Castellanos-Gomez, A., Molybdenum Oxides - From Fundamentals to Functionality. *Adv Mater* **2017,** *29* (40).
10. Ellefson, C. A.; Marin-Flores, O.; Ha, S.; Norton, M. G., Synthesis and applications of molybdenum (IV) oxide. *J. Mater. Sci.* **2012,** *47* (5), 2057-2071.

11. Proust, A.; Thouvenot, R.; Gouzerh, P., Functionalization of polyoxometalates: towards advanced applications in catalysis and materials science. *Chem. Commun. (Cambridge, U. K.)* **2008,** (16), 1837-1852.
12. Ren, H.; Sun, S.; Cui, J.; Li, X., Synthesis, Functional Modifications, and Diversified Applications of Molybdenum Oxides Micro-/Nanocrystals: A Review. *Cryst. Growth Des.* **2018,** *18* (10), 6326-6369.
13. Saji, V. S.; Lee, C.-W., Molybdenum, Molybdenum Oxides, and their Electrochemistry. *ChemSusChem* **2012,** *5* (7), 1146-1161.
14. Zharikov, E. V.; Zaldo, C.; Diaz, F., Double tungstate and molybdate crystals for laser and nonlinear optical applications. *MRS Bull.* **2009,** *34* (4), 271-276.
15. Saito, M.; Anderson, R., The activity of several molybdenum compounds for the methanation of CO. *Journal of catalysis* **1980,** *63* (2), 438-446.
16. Lacorre, P.; Goutenoire, F.; Bohnke, O.; Retoux, R.; Laligant, Y., Designing fast oxide-ion conductors based on La2Mo2O 9. *Nature* **2000,** *404*, 856.
17. Arulraj, A.; Goutenoire, F.; Tabellout, M.; Bohnke, O.; Lacorre, P., Synthesis and Characterization of the Anionic Conductor System La2Mo2O9-0.5xFx (x = 0.02-0.30). *Chem. Mater.* **2002,** *14* (6), 2492-2498.
18. Basu, S.; Devi, P. S.; Maiti, H. S.; Bandyopadhyay, N. R., Synthesis, thermal and electrical analysis of alkaline earth doped lanthanum molybdate. *Solid State Ionics* **2013,** *231*, 87-93.
19. Corbel, G.; Durand, P.; Lacorre, P., Comprehensive survey of Nd3+ substitution in La2Mo2O9 oxide-ion conductor. *J. Solid State Chem.* **2009,** *182* (5), 1009-1016.
20. Goel, M.; Djurado, E.; Georges, S., Reducibility of La2Mo2O9 based ceramics versus porosity. *Solid State Ionics* **2011,** *204-205*, 97-103.
21. Goutenoire, F.; Isnard, O.; Retoux, R.; Lacorre, P., Crystal structure of La2Mo2O9, a new fast oxide-ion conductor. *Chem. Mater.* **2000,** *12* (9), 2575-2580.
22. Lacorre, P.; Goutenoire, F.; Altorfer, F.; Sheptyakov, D.; Fauth, F.; Suard, E., Crystal structure of new fast oxide-ion conductor La2Mo2O9. *Adv. Sci. Technol. (Faenza, Italy)* **2003,** *33* (10th International Ceramics Congress, 2002, Part D), 737-747.
23. Le, M.-V.; Tsai, D.-S.; Yao, C.-C.; Lo, J.-C.; Vo, T. P. G., Properties of 10% Dy-doped La2Mo2O9 and its electrolyte performance in single chamber solid oxide fuel cell. *J. Alloys Compd.* **2014,** *582*, 780-785.
24. Malavasi, L.; Kim, H.; Billinge, S. J. L.; Proffen, T.; Tealdi, C.; Flor, G., Nature of the monoclinic to cubic phase transition in the fast oxygen ion conductor La2Mo2O9 (LAMOX). *J. Am. Chem. Soc.* **2007,** *129* (21), 6903-6907.
25. Sellemi, H.; Coste, S.; Ben Ali, A.; Retoux, R.; Smiri, L. S.; Lacorre, P., Synthesis of La2Mo2O9 powders with nanodomains using polyol procedure. *Ceram. Int.* **2013,** *39* (8), 8853-8859.
26. Tealdi, C.; Chiodelli, G.; Malavasi, L.; Flor, G., Effect of alkaline doping on the properties of La2Mo2O9 fast oxygen ion conductor. *J. Mater. Chem.* **2004,** *14* (24), 3553-3557.
27. Vega-Castillo, J.; Mogni, L.; Corbel, G.; Lacorre, P.; Caneiro, A., On the thermodynamic stability of La2Mo2O9-δ oxide-ion conductor. *Int. J. Hydrogen Energy* **2010,** *35* (11), 5890-5894.

28. Voronkova, V. I.; Kharitonova, E. P., Oxygen-conducting compounds with La2Mo2O9 structure in the ternary system La2Mo2O9-Sm2W2O9-Sm2Mo2O+9: Synthesis and properties. *Crystallogr. Rep.* **2014,** *59* (4), 574-579.
29. Wang, J. X.; Wang, X. P.; Liang, F. J.; Cheng, Z. J.; Fang, Q. F., Enhancement of conductivity in La2Mo2O9 ceramics fabricated by a novel three-stage thermal processing method. *Solid State Ionics* **2006,** *177* (17-18), 1437-1442.
30. Apblett, A. W.; Chehbouni, M.; Reinhardt, L. E., Novel routes to ferroelectric gadolinium molybdenum oxides. *Ceram. Trans.* **2006,** *174* (Advances in Dielectric Materials and Electronic Devices), 39-46.
31. Chehbouni, M. Environmental, synthetic, and materials applications of molybdenum trioxide. Ph.D. Dissertation, Oklahoma State University, 2006.
32. Chehbouni, M.; Al-Busaidi, H.; Apblett, A. W., Green process for uranium separations utilizing molybdenum trioxide. *ACS Symp. Ser.* **2010,** *1046* (Nuclear Energy and the Environment), 155-167.
33. Chehbouni, M.; Apblett, A. W., Molybdenum-oxide based sorbents for toxic metals. *Ceram. Trans.* **2006,** *176* (Environmental Issues and Waste Management Technologies in the Ceramic and Nuclear Industries XI), 15-23.
34. Cortese, A. J.; Abeysinghe, D.; Wilkins, B.; Smith, M. D.; Morrison, G.; zur Loye, H.-C., High-Temperature Salt Flux Crystal Growth of New Lanthanide Molybdenum Oxides, Ln5Mo2O12 Ln = Eu, Tb, Dy, Ho, and Er: Magnetic Coupling within Mixed Valent Mo(IV/V) Rutile-Like Chains. *Inorg. Chem.* **2015,** *54* (24), 11875-11882.
35. Cortese, A. J.; Abeysinghe, D.; Wilkins, B.; Smith, M. D.; Rassolov, V.; zur Loye, H.-C., Oxygen Anion Solubility as a Factor in Molten Flux Crystal Growth, Synthesis, and Characterization of Four New Reduced Lanthanide Molybdenum Oxides: Ce4.918(3)Mo3O16, Pr4.880(3)Mo3O16, Nd4.910(3)Mo3O16, and Sm4.952(3)Mo3O16. *Cryst. Growth Des.* **2016,** *16* (8), 4225-4231.
36. Eda, K.; Kunotani, F.; Uchiyama, N., Low-temperature synthetic route based on the amorphous nature of giant species for preparation of lower valence oxides. *J. Solid State Chem.* **2005,** *178* (5), 1471-1477.
37. Miura, M.; Wakeshima, M.; Hinatsu, Y., Crystal structures and magnetic properties of Ln5Mo2O12 (Ln = Y, Dy-Lu). *Kidorui* **2015,** *66*, 158-159.
38. Safronenko, M. G.; Bogatov, Y. E.; Tkachenko, E. A.; Sakharova, O. V., Study of a possibility for the synthesis of molybdates, Ln3MoO7. *Zh. Neorg. Khim.* **1997,** *42* (4), 519-520.
39. Shi, F.; Meng, J.; Ren, Y., Preparation structure and physical properties of new silver lanthanide molybdenum oxides [AgLnMo2O8 (Ln = La-Nd and Sm)]. *Mater. Res. Bull.* **1995,** *30* (11), 1401-5.
40. Shi, F.; Ren, Y.; Meng, J., Preparation, structure, electrical and magnetic properties of Ln2Mo3O9. *Yingyong Huaxue* **1995,** *12* (2), 95-7.
41. Tkachenko, E. A.; Bogatov, Y. E.; Kurilkin, V. V., Interactions of rare-earth molybdates(V) of composition LnMoO4 (Ln = La, Nd, Gd, Dy, Er) with sulfur. *Zh. Neorg. Khim.* **2004,** *49* (4), 559-567.
42. Xu, J.-X.; Sonne, M.; Yanangiya, S.-I.; Nong, N.-V.; Pryds, N.; Nygren, M.; Kleinke, H., High thermoelectric performance of reduced lanthanide molybdenum oxides densified by spark plasma sintering. *J. Alloys Compd.* **2010,** *500* (1), 22-25.

43. Shannon, R. D., Revised effective ionic radii and systematic studies of interatomic distances in halides and chalcogenides. *Acta crystallographica section A: crystal physics, diffraction, theoretical and general crystallography* **1976,** *32* (5), 751-767.
44. Chehbouni, M. Environmental, synthetic, and materials applications of molybdenum trioxide. Ph.D., Oklahoma State University, Ann Arbor, 2006.
45. Chen, Y.; Liang, Y.; Cai, M.; Ke, T.; Zhang, M.; He, X.; Zeng, Q., Luminescent property and application research of red molybdate phosphors for W-LEDs. *J. Mater. Sci.: Mater. Electron.* **2018,** *29* (14), 11930-11935.
46. Dai, P., Enhanced red emission induced by Tb3+ doping in europium-based molybdate phosphors. *Mater. Res. Bull.* **2017,** *94*, 64-69.
47. Jin, Y.; Zhang, J.; Lue, S.; Zhao, H.; Zhang, X.; Wang, X.-j., Fabrication of Eu3+ and Sm3+ Codoped Micro/Nanosized MMoO4 (M = Ca, Ba, and Sr) via Facile Hydrothermal Method and Their Photoluminescence Properties through Energy Transfer. *J. Phys. Chem. C* **2008,** *112* (15), 5860-5864.
48. Lee, G.-H.; Kang, S.-H., Solid-solution red phosphors for white LEDs. *J. Lumin.* **2011,** *131* (12), 2582-2588.
49. Tawalare, P. K.; Bhatkar, V. B.; Talewar, R. A.; Joshi, C. P.; Moharil, S. V., Host sensitized NIR emission in rare-earth doped NaY(MoO4)2 phosphors. *J. Alloys Compd.* **2018,** *732*, 64-69.
50. Xie, A.; Yang, W. Y.; Zhang, M. S., Red emitting tungsto-molybdate phosphor for near-ultraviolet light-emitting diodes-based solid-state lighting. *Sci. China: Phys., Mech. Astron.* **2012,** *55* (7), 1229-1234.
51. Zhai, Y.-Q.; Ma, J.; Hu, Z.-C.; Zhao, J.-J.; Yang, M.-Y.; Zhao, L., Preparation and enhancement of luminescent intensity of new rare earth molybdate NaLa(MoO4)2:Eu3+ phosphors. *Asian J. Chem.* **2014,** *26* (11), 3129-3133.
52. Zhang, Z.; Yang, Y.; Li, W., Synthesis and luminescent properties of Eu3+ doped double molybdate phosphors. *Adv. Mater. Res. (Zuerich, Switz.)* **2011,** *211-212* (Pt. 1, Mechanotronics and Intelligent Materials), 213-216.
53. Rodriguez, J. A.; Hanson, J. C.; Chaturvedi, S.; Maiti, A.; Brito, J. L., Phase transformations and electronic properties in mixed-metal oxides: Experimental and theoretical studies on the behavior of NiMoO 4 and MgMoO 4. *The Journal of Chemical Physics* **2000,** *112* (2), 935-945.
54. Wells, A. F., *Structural inorganic chemistry*. Oxford university press: 2012.
55. Davolos, M. R.; Feliciano, S.; Pires, A. M.; Marques, R. F. C.; Jafelicci, M., Solvothermal method to obtain europium-doped yttrium oxide. *Journal of Solid State Chemistry* **2003,** *171* (1-2), 268-272.
56. Eda, K.; Uno, Y.; Nagai, N.; Sotani, N.; Whittingham, M. S., Crystal structure of cobalt molybdate hydrate CoMoO 4· nH 2 O. *Journal of Solid State Chemistry* **2005,** *178* (9), 2791-2797.

VITA

KHALID ABDULLAH ALRASHIDI
Degree of Master

Thesis: SYNTHESIS OF LANTHANIDE MOLYBDATES VIA REACTION OF MOLYBDENUM(VI) OXIDE WITH AQUEOUS ACETATE SALTS.

Major Field: CHEMISTRY: Completed the requirements for the Master Degree in Inorganic Chemistry at Oklahoma State University, Stillwater, Oklahoma in December, 2018.

Education:

Completed the requirements for the Bachelor of Science Chemistry at King Saud University, Riyadh, Saudi Arabia in 2011.

Experience: Employed by King Saud University, Riyadh, Kingdom of Saudi Arabia as a teaching assistant from 2012 to 2016.

Abstracts:

Reaction of aqueous solutions of either lanthanum or cerium acetate with molybdenum(VI) oxide (MoO_3) produces a mixed lanthanide molybdate acetate, $Ln(O_2CCH_3(MoO_4)\bullet XH_2O$ (Ln= La, Ce) that is an excellent single source precursor for stoichiometric $Ln_2Mo_2O_9$. The reaction is very sensitive to the radius of the lanthanide metal used: metals with smaller radii (e.g. yttrium, praseodymium or neodymium) produce a hydroxyl molybdate product, $M(OH)_x(MoO_4)_{1-x}$, instead of an acetate molybdate. The products were fired at high temperatures for further investigation. The products were characterized by thermal gravimetric analysis (TGA) and infrared and NMR spectroscopy. The conversion of the products to lanthanide molybdenum oxides was used to study the possibility of producing phosphors, $La_2Mo_2O_9:Ln^{3+}$ by doping lanthanum molybdenum oxides with other lanthanide metals such as praseodymium acetate. Also, fluorescence spectroscopy was run to study the doping material.